AIP Applied Physics Letters

Large optical gain AlGaN-delta-GaN quantum wells laser active regions in mid- and deep-ultraviolet spectral regimes

Jing Zhang, Hongping Zhao, and Nelson Tansu

Citation: Appl. Phys. Lett. 98, 171111 (2011); doi: 10.1063/1.3583442

View online: http://dx.doi.org/10.1063/1.3583442

View Table of Contents: http://apl.aip.org/resource/1/APPLAB/v98/i17

Published by the American Institute of Physics.

Large optical gain AlGaN-delta-GaN quantum wells laser active regions in mid- and deep-ultraviolet spectral regimes

Jing Zhang,[a)] Hongping Zhao, and Nelson Tansu[b)]
Department of Electrical and Computer Engineering, Center for Optical Technologies, Lehigh University, Bethlehem, Pennsylvania 18015, USA

(Received 18 February 2011; accepted 7 April 2011; published online 28 April 2011)

The gain characteristics of high Al-content AlGaN-delta-GaN quantum wells (QWs) are investigated for mid- and deep-ultraviolet (UV) lasers. The insertion of an ultrathin GaN layer in high Al-content AlGaN QWs leads to valence subbands rearrangement, which in turn results in large optical gain for mid- and deep-UV lasers. © *2011 American Institute of Physics*. [doi:10.1063/1.3583442]

Nitride semiconductors have important applications for lasers and light-emitting diodes (LEDs),[1–11] power electronics,[12] thermoelectricity,[13–15] solar cells,[16] and terahertz photonics.[17] The electrically-injected AlGaN quantum wells (QWs) lasers have been realized in the emission wavelength $(\lambda) \sim 320-360$ nm.[18–33] Up to today, no electrically injected mid-$(\lambda \sim 250-320$ nm) and deep-ultraviolet (UV) $(\lambda \sim 220-250$ nm) lasers have been realized. Recent theoretical works have been reported on the gain properties for both low[36–38] and high Al-content[34,39] AlGaN QWs while the detailed studies on gain properties of high Al-content AlGaN QWs are still lacking.

Our recent work[34] revealed that the use of high Al-content AlGaN QWs resulted in strong conduction (C)-crystal-field split-off hole (CH) transition, which led to large transverse-magnetic (TM)-polarized gain for $\lambda \sim 220-230$ nm. The large TM-polarized gain in high Al-content (>68%) AlGaN QW was attributed to the dominant C-CH transition.[34] Recent experiments also confirmed that TM-polarized emission was dominant for higher Al-content AlGaN QWs LEDs,[35] in agreement with our prediction.[34]

In this letter, we present the gain properties of high Al-content (x) $Al_xGa_{1-x}N$-delta-GaN QW with large transverse-electric (TE) polarized gain at $\lambda \sim 220-300$ nm. The delta QW is realized by the insertion of GaN delta-layer (3–9 Å) in high Al-content AlGaN QW leading to strong valence subbands mixing. The band structures and wave functions were calculated based on 6-band $\boldsymbol{k}\cdot\boldsymbol{p}$ formalism taking into account the valence band mixing, strain, polarization fields, and carrier screening effects,[40–44] with the band parameters obtained from Refs. 44–46.

Figure 1 shows the material gains calculated for 3 nm conventional $Al_xGa_{1-x}N$ QW with AlN barriers with $x = 20\%-80\%$. Large TM-polarized material gains (g_{peak}^{TM}) are achievable for $Al_xGa_{1-x}N$ QWs with $x=70\%$ and 80% $(\lambda_{peak} \sim 220-230$ nm), while the corresponding TE gains are relatively low. In addition, the conventional $Al_xGa_{1-x}N$ QWs in the 250–320 nm spectral range are limited to relatively low TE and TM gains for Al-contents below 60% (Fig. 1). The low gain for the AlGaN QW in the $\sim 250-320$ nm spectral regime is attributed to the significant band filling for the heavy-hole (HH)/light-hole (LH) and CH subbands.[34] Thus, the pursuit of mid-UV AlGaN-based QW with large gain is of great importance for lasers. The availability of large TE-gain deep-UV QW is also important for laser structures that require high TE gain.

By employing the AlGaN-delta-GaN QW [Fig. 2(b)], the strong valence band mixing results in the valence subband rearrangement, which in turn leads to (1) higher HH1 and LH1 subband energy levels in comparison to that of the CH1 subband, (2) splitting of the HH1 and LH1 subbands, and (3) dominant C1-HH1 transition leading to large TE gain. Thus, large TE gains in the deep- and mid-UV spectral regimes are achievable with the AlGaN-delta-GaN QW.

Figures 2(a) and 2(b) show the valence band structures for both conventional 30 Å $Al_{0.8}Ga_{0.2}N$ QW and 30 Å $Al_{0.8}Ga_{0.2}N/3$ Å GaN QW, respectively, for $n=5 \times 10^{19}$ cm^{-3} at T=300 K. All structures studied here employed AlN barriers. For conventional $Al_{0.8}Ga_{0.2}N$ QW, the CH1 subband energy is much larger than those of the HH1 and LH1 subbands [Fig. 2(a)]. In contrast, the HH1 and LH1 subbands are rearranged into higher subband energy levels than that of the CH1 subband for the 30 Å $Al_{0.8}Ga_{0.2}N/3$ Å GaN QW (delta-QW). The energy separation between the HH1 and CH1 subbands for the $Al_{0.8}Ga_{0.2}N/3$ Å GaN QW is relatively large (~ 140 meV) at Γ-point [Fig. 2(b)], which results in dominant C1-HH1 transition.

Figure 3(a) shows both the TE and TM optical gain spectra for 30 Å $Al_xGa_{1-x}N/3$ Å GaN QW $(x=0.7, 0.8)$ with $n = 5 \times 10^{19}$ cm^{-3} at T=300 K. Attributing to the insertion of the GaN delta-layer into $Al_xGa_{1-x}N$ QW, the band energies of HH and LH subbands are increased significantly than that

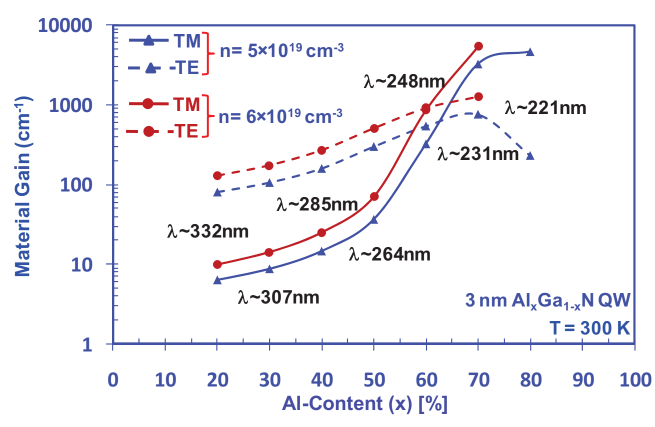

FIG. 1. (Color online) TE and TM material gains as a function of Al-content (x) for 3 nm $Al_xGa_{1-x}N$ QW with AlN barriers for $n=5 \times 10^{19}$ cm^{-3} and 6×10^{19} cm^{-3}, with the emission wavelengths (λ) at $n=5 \times 10^{19}$ cm^{-3}.

[a)]Electronic mail: jiz209@lehigh.edu.
[b)]Electronic mail: tansu@lehigh.edu.

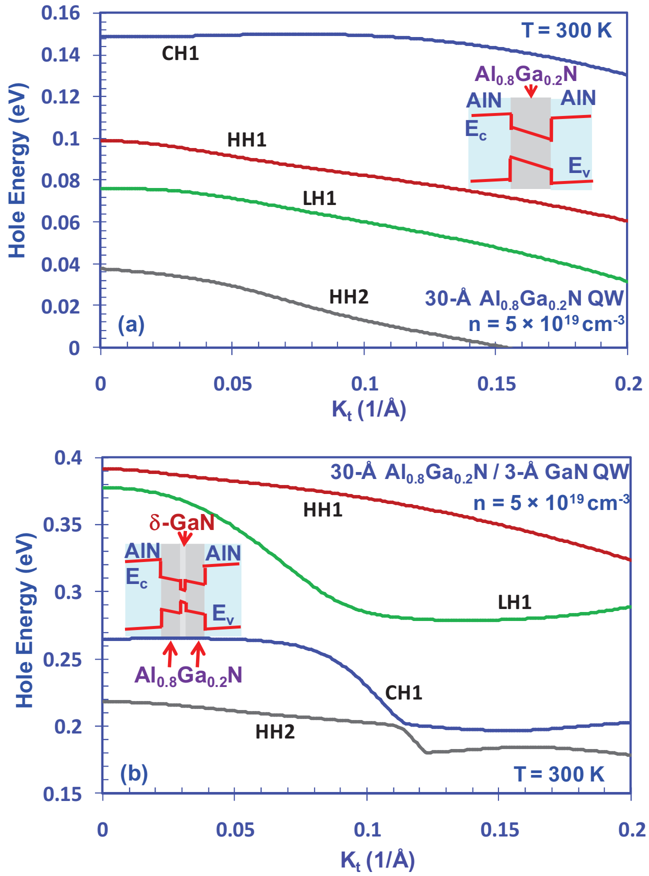

FIG. 2. (Color online) The schematics and the valence band structures of (a) conventional 30 Å $Al_{0.8}Ga_{0.2}N$ QW and (b) 30 Å $Al_{0.8}Ga_{0.2}N$/3 Å GaN QW with AlN barriers.

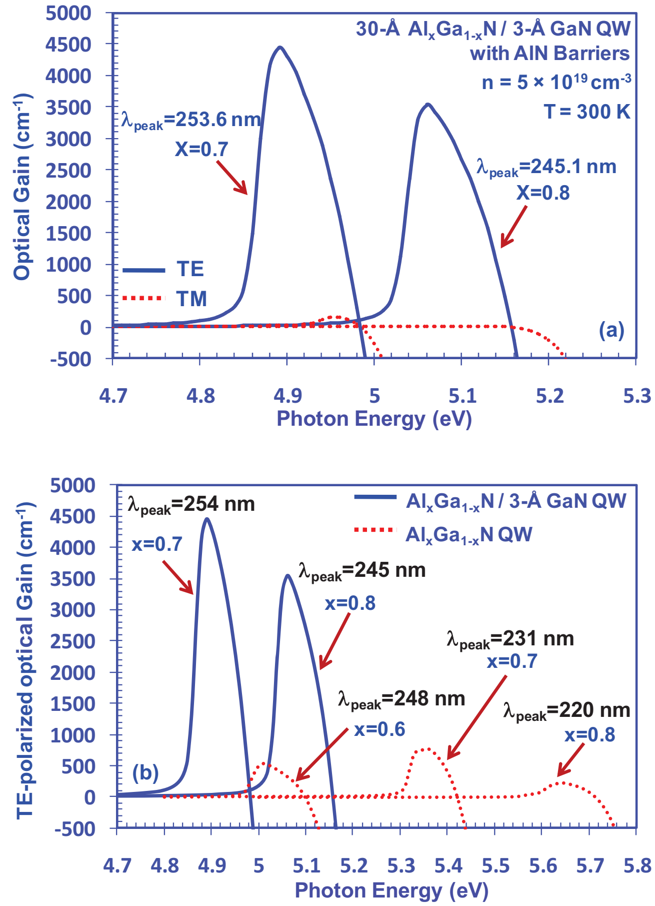

FIG. 3. (Color online) (a) TE and TM gain spectra for 30 Å $Al_{0.8}Ga_{0.2}N$/3 Å GaN QW and (b) TE gain spectra for both 30 Å $Al_xGa_{1-x}N$/3 Å GaN QW and conventional $Al_xGa_{1-x}N$ QW with AlN barriers.

of the CH subband. Thus, the TE gains for both 30 Å $Al_{0.7}Ga_{0.3}N$/3 Å GaN QW and 30-Å $Al_{0.8}Ga_{0.2}N$/3-Å GaN QW become dominant ($g^{TE}_{peak}=4442$ cm^{-1} for $x=0.7$, and $g^{TE}_{peak}=3537$ cm^{-1} for $x=0.8$) while the TM gains are negligible as compared to the TE gains.

Figure 3(b) shows the comparison of the TE optical gains for 30 Å $Al_xGa_{1-x}N$/3 Å GaN QW ($x=0.7,0.8$) and conventional 30 Å $Al_xGa_{1-x}N$ QW ($x=0.6,0.7,0.8$) for $n=5\times10^{19}$ cm^{-3} at T=300 K. For conventional $Al_xGa_{1-x}N$ QW, relatively low TE gains ($g^{TE}_{peak}=539$ cm^{-1} for $x=0.6$; $g^{TE}_{peak}=763$ cm^{-1} for $x=0.7$; $g^{TE}_{peak}=232$ cm^{-1} for $x=0.8$) were obtained with $\lambda_{peak}\sim220-250$ nm. In contrast, large TE gains were obtained with $\lambda_{peak}\sim245-255$ nm for gain media employing $Al_xGa_{1-x}N$ delta-GaN QWs. For $Al_{0.7}Ga_{0.3}N$/3 Å GaN and $Al_{0.8}Ga_{0.2}N$/3 Å GaN QW, the TE gains are 4442 and 3537 cm^{-1} for $\lambda_{peak}=253.6$ nm and $\lambda_{peak}=245.1$ nm, respectively.

Figure 4(a) shows the TE gain spectra for AlGaN-delta-GaN QW as a function of GaN delta-layer thickness (d) with $n=5\times10^{19}$ cm^{-3} at $T=300$ K. For GaN delta-layer thickness ≤ 9 Å (as delta layer), high TE gain can be obtained from the insertion of the delta layer attributed to the HH/CH band realignment in the QW. The use of the delta layer in the QW pushes the CH1 subband further away from the valence band edge [Fig. 2(b)], which leads to the C1-HH1 dominant transition. For GaN layer thickness >9 Å, the TE gain decreases severely with larger GaN thickness, which indicates that the GaN layer behaves as single QW-like active region. Thus, the use of AlGaN-delta-GaN QW leads to high gain material for $\lambda_{peak}\sim240-300$ nm, as well as large TE gain in the deep UV spectral regime.

Figure 4(b) shows the TE material gain as a function of carrier density at $T=300$ K for 30 Å $Al_{0.7}Ga_{0.3}N$/9 Å GaN QW, 30 Å $Al_xGa_{1-x}N$/3 Å GaN QW ($x=0.7,0.8$), and conventional 30 Å $Al_xGa_{1-x}N$ QW ($x=0.7,0.8$). The 30 Å $Al_{0.7}Ga_{0.3}N$/9 Å GaN QW shows transparency carrier density (n_{tr}) as $n_{tr}\sim1.0\times10^{19}$ cm^{-3}, and the $n_{tr}\sim1.8\times10^{19}$ cm^{-3} are obtained for both 30 Å $Al_{0.7}Ga_{0.3}N$/3 Å GaN QW and 30 Å $Al_{0.8}Ga_{0.2}N$/3-Å GaN QW. All the delta QW gain media exhibit significantly higher TE materials gains, in comparison to those of conventional AlGaN QWs [Fig. 4(b)]. For $n>4\times10^{19}$ cm^{-3}, the TE material gain for $Al_{0.7}Ga_{0.3}N$/3 Å GaN QW is $\sim$1.05–1.26 times of the $Al_{0.8}Ga_{0.2}N$/3 Å GaN QW, which is attributed from better carrier confinement that leads to larger momentum matrix element. In comparison to the conventional 30 Å $Al_{0.7}Ga_{0.3}N$ QW, the insertion of 3 and 9 Å GaN delta-layer in the 30 Å $Al_{0.7}Ga_{0.3}N$ QW active regions lead to increase in TE gain up to $\sim$5.8 times and $\sim$6.0 times while the increase in TE gain is $\sim$15.3 times for 30 Å $Al_{0.8}Ga_{0.2}N$/3-Å GaN QW in comparison to that of conventional 30 Å $Al_{0.8}Ga_{0.2}N$ QW.

The threshold properties of AlGaN-delta-GaN QW were analyzed. The laser structure ($L_{cav}=500$ μm) with optical confinement factor of 0.02 (Ref. 37) and mirror loss of 11 cm^{-1} was used, and the internal loss was 50 cm^{-1}.[37] The threshold gain (g_{th}) was $\sim$3050 cm^{-1}. From Fig. 4(b), the threshold carrier densities (n_{th}) are 4.4×10^{19} cm^{-3} and 4.2

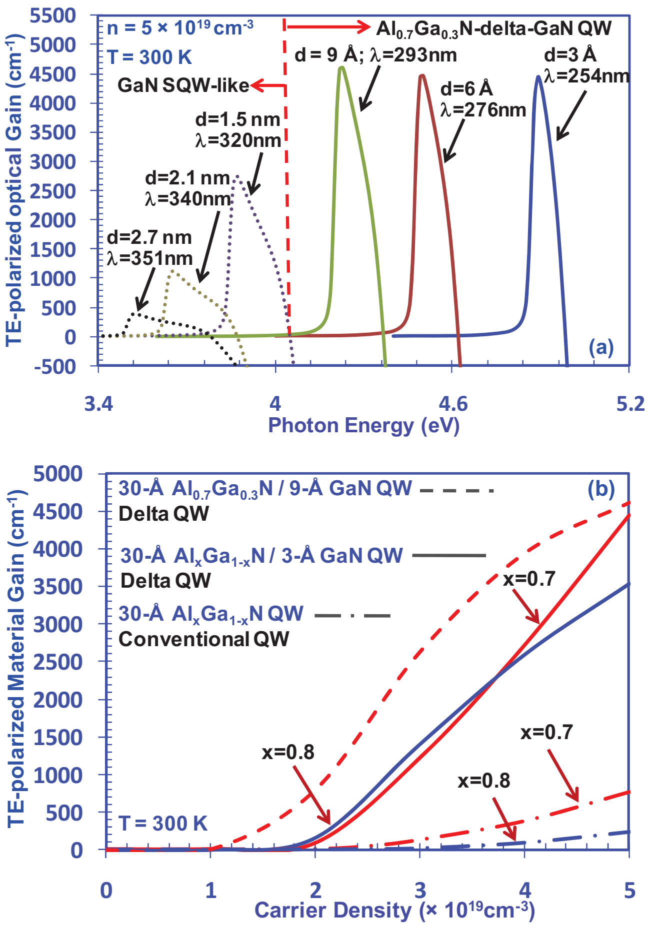

FIG. 4. (Color online) (a) TE optical gain for 30 Å $Al_{0.7}Ga_{0.3}N/d$ Å GaN QW at $n=5\times10^{19}$ cm^{-3} and (b) TE material gain as a function of carrier density for 30 Å $Al_{0.7}Ga_{0.3}N/9$ Å GaN QW, 30 Å $Al_xGa_{1-x}N/3$ Å GaN QW ($x=0.7,0.8$), and 30 Å $Al_xGa_{1-x}N$ QW ($x=0.7,0.8$).

$\times10^{19}$ cm^{-3} for $Al_{0.8}Ga_{0.2}N/3$ Å GaN QW ($\lambda\sim245$ nm) and $Al_{0.7}Ga_{0.3}N/3$ Å GaN QW ($\lambda\sim254$ nm), respectively. For mid UV lasers ($\lambda\sim293$ nm) using $Al_{0.7}Ga_{0.3}N/9$ Å GaN QW, the n_{th} is 3.3×10^{19} cm^{-3}.

In summary, the gain characteristics of high Al-content AlGaN-delta-GaN QWs were analyzed for mid- and deep-UV lasers. Attributing to the strong transition between the C1-HH1 subbands, high TE gain is achievable for high Al-content AlGaN-delta-GaN QWs as active regions for mid- and deep-UV lasers.

The work is supported by U.S. National Science Foundation (Grant Nos. ECCS 0701421 and ECCS 1028490), and Class of 1961 Professorship Fund.

[1] R. M. Farrell, D. F. Feezell, M. C. Schmidt, D. A. Haeger, K. M. Kelchner, K. Iso, H. Yamada, M. Saito, K. Fujito, D. A. Cohen, J. S. Speck, S. P. DenBaars, and S. Nakamura, Jpn. J. Appl. Phys., Part 2 **46**, L761 (2007).
[2] M. H. Kim, M. F. Schubert, Q. Dai, J. K. Kim, E. F. Schubert, J. Piprek, and Y. Park, Appl. Phys. Lett. **91**, 183507 (2007).
[3] H. Zhao, J. Zhang, G. Liu, and Tansu Appl. Phys. Lett. **98**, 151115 (2011).
[4] Y. K. Ee, P. Kumnorkaew, R. A. Arif, H. Tong, H. Zhao, J. F. Gilchrist, and N. Tansu, IEEE J. Sel. Top. Quantum Electron. **15**, 1218 (2009).
[5] Y. K. Ee, J. M. Biser, W. Cao, H. M. Chan, R. P. Vinci, and N. Tansu, IEEE J. Sel. Top. Quantum Electron. **15**, 1066 (2009).
[6] S. H. Park, D. Ahn, B. H. Koo, and J. W. Kim, Appl. Phys. Lett. **95**, 063507 (2009).
[7] C. T. Liao, M. C. Tsai, B. T. Liou, S. H. Yen, and Y. K. Kuo, J. Appl. Phys. **40**, 301 (2008).
[8] H. Zhao, G. Liu, X. H. Li, G. S. Huang, J. D. Poplawsky, S. Tafon Penn, V. Dierolf, and N. Tansu, Appl. Phys. Lett. **95**, 061104 (2009).
[9] H. P. Zhao, G. Y. Liu, X. H. Li, R. A. Arif, G. S. Huang, J. D. Poplawsky, S. Tafon Penn, V. Dierolf, and N. Tansu, IET Optoelectron. **3**, 283 (2009).
[10] Y. K. Ee, P. Kumnorkaew, R. A. Arif, H. Tong, J. F. Gilchrist, and N. Tansu, Opt. Express **17**, 13747 (2009).
[11] H. Zhao, G. Liu, R. A. Arif, and N. Tansu, Solid-State Electron. **54**, 1119 (2010).
[12] U. K. Mishra, P. Parikh, and Y. F. Wu, Proc. IEEE **90**, 1022 (2002).
[13] B. N. Pantha, R. Dahal, J. Li, J. Y. Lin, H. X. Jiang, and G. Pomrenke, Appl. Phys. Lett. **92**, 042112 (2008).
[14] H. Tong, J. Zhang, G. Liu, J. A. Herbsommer, G. S. Huang, and N. Tansu, Appl. Phys. Lett. **97**, 112105 (2010).
[15] J. Zhang, H. Tong, G. Y. Liu, J. A. Herbsommer, G. S. Huang, and N. Tansu, J. Appl. Phys. **109**, 053706 (2011).
[16] M. Jamil, H. Zhao, J. Higgins, and N. Tansu, Phys. Status Solidi A **205**, 2886 (2008).
[17] G. Sun, G. Xu, Y. J. Ding, H. Zhao, G. Liu, J. Zhang, and N. Tansu, IEEE J. Sel. Top. Quantum Electron. **17**, 48 (2011).
[18] A. Yasan, R. McClintock, K. Mayes, D. Shiell, L. Gautero, S. R. Darvish, P. Kung, and M. Razeghi, Appl. Phys. Lett. **83**, 4701 (2003).
[19] A. J. Fischer, A. A. Allerman, M. H. Crawford, K. H. A. Bogart, S. R. Lee, R. J. Kaplar, W. W. Chow, S. R. Kurtz, K. W. Fullmer, and J. J. Figiel, Appl. Phys. Lett. **84**, 3394 (2004).
[20] V. Adivarahan, S. Wu, J. P. Zhang, A. Chitnis, M. Shatalov, V. Mandavilli, R. Gaska, and M. A. Khan, Appl. Phys. Lett. **84**, 4762 (2004).
[21] Z. Ren, Q. Sun, S. Y. Kwon, J. Han, K. Davitt, Y. K. Song, A. V. Nurmikko, H. K. Cho, W. Liu, J. A. Smart, and L. J. Schowalter, Appl. Phys. Lett. **91**, 051116 (2007).
[22] A. V. Sampath, M. L. Reed, C. Chua, G. A. Garrett, G. Dang, E. D. Readinger, H. Shen, A. Usikov, O. Kovalenkov, L. Shapovalova, V. A. Dmitriev, N. M. Johnson, and M. Wraback, Phys. Status Solidi C **5**, 2303 (2008).
[23] C. G. Moe, M. L. Reed, G. A. Garrett, A. V. Sampath, T. Alexander, H. Shen, M. Wraback, Y. Bilenko, M. Shatalov, J. Yang, W. Sun, J. Deng, and R. Gaska, Appl. Phys. Lett. **96**, 213512 (2010).
[24] Y. Sakai, Y. Zhu, S. Sumiya, M. Miyoshi, M. Tanaka, and T. Egawa, Jpn. J. Appl. Phys. **49**, 022102 (2010).
[25] Y. Taniyasu and M. Kasu, Appl. Phys. Lett. **96**, 221110 (2010).
[26] H. Hirayama, N. Noguchi, and N. Kamata, Appl. Phys. Express **3**, 032102 (2010).
[27] T. Takano, Y. Narita, A. Horiuchi, and H. Kawanishi, Appl. Phys. Lett. **84**, 3567 (2004).
[28] M. Kneissl, Z. Yang, M. Teepe, C. Knollenberg, O. Schmidt, P. Kiesel, N. M. Johnson, S. Schujman, and L. J. Schowalter, J. Appl. Phys. **101**, 123103 (2007).
[29] V. N. Jmerik, A. M. Mizerov, A. A. Sitnikova, P. S. Kop'ev, S. V. Ivanov, E. V. Lutsenko, N. P. Tarasuk, N. V. Rzheutskii, and G. P. Yablonskii, Appl. Phys. Lett. **96**, 141112 (2010).
[30] H. Yoshida, M. Kuwabara, Y. Yamashita, K. Uchiyama, and H. Kan, Appl. Phys. Lett. **96**, 211122 (2010).
[31] H. Yoshida, M. Kuwabara, Y. Yamashita, Y. Takagi, K. Uchiyama, and H. Kan, N. J. Phys. **11**, 125013 (2009).
[32] M. Kneissl, D. W. Treat, M. Teepe, N. Miyashita, and N. M. Johnson, Appl. Phys. Lett. **82**, 2386 (2003).
[33] C. Chen, M. Shatalov, E. Kuokstis, V. Adivarahan, M. Gaevski, S. Rai, and M. Asif Khan, Jpn. J. Appl. Phys., Part 2 **43**, L1099 (2004).
[34] J. Zhang, H. Zhao, and N. Tansu, Appl. Phys. Lett. **97**, 111105 (2010).
[35] T. Kolbe, A. Knauer, C. Chua, Z. Yang, S. Einfeldt, P. Vogt, N. M. Johnson, M. Weyers, and M. Kneissl, Appl. Phys. Lett. **97**, 171105 (2010).
[36] W. W. Chow, M. Kneissl, J. E. Northrup, and N. M. Johnson, Appl. Phys. Lett. **90**, 101116 (2007).
[37] W. W. Chow and M. Kneissl, J. Appl. Phys. **98**, 114502 (2005).
[38] S. H. Park and S. L. Chuang, Appl. Phys. A: Mater. Sci. Process. **78**, 107 (2004).
[39] S. H. Park, Semicond. Sci. Technol. **24**, 035002 (2009).
[40] S. L. Chuang, IEEE J. Quantum Electron. **32**, 1791 (1996).
[41] S. L. Chuang and C. S. Chang, Semicond. Sci. Technol. **12**, 252 (1997).
[42] S. L. Chuang, *Physics of Photonic Devices*, 2nd ed. (Wiley, New York, 2009), Chap. 4.
[43] H. Zhao, R. A. Arif, Y. K. Ee, and N. Tansu, IEEE J. Quantum Electron. **45**, 66 (2009).
[44] H. Zhao and N. Tansu, J. Appl. Phys. **107**, 113110 (2010).
[45] I. Vurgaftman and J. R. Meyer, in *Nitride Semiconductor Devices*, edited by J. Piprek (Wiley, New York, 2007), Chap. 2.
[46] I. Vurgaftman and J. R. Meyer, J. Appl. Phys. **94**, 3675 (2003).